THE JOURNAL OF BIOLOGICAL CHEMISTRY
Vol. 278, No. 41, Issue of October 10, pp. 39697–39705, 2003

Printed in U.S.A.

Characterization of 2′-Fluoro-RNA Aptamers That Bind Preferentially to Disease-associated Conformations of Prion Protein and Inhibit Conversion*

Received for publication, May 20, 2003, and in revised form, July 30, 2003
Published, JBC Papers in Press, August 5, 2003, DOI 10.1074/jbc.M305297200

Alexandre Rhie‡§, Louise Kirby§, Natalie Sayer‡, Rosanna Wellesley‡, Petra Disterer‡, Ian Sylvester§, Andrew Gill§, James Hope§¶, William James‡‖, and Abdessamad Tahiri-Alaoui‡**

From the ‡Sir William Dunn School of Pathology, University of Oxford, South Parks Road, Oxford OX1 3RE, United Kingdom and the §Institute for Animal Health, Compton, Berkshire, Newbury RG20 7NN, United Kingdom

We have isolated artificial ligands or aptamers for infectious prions in order to investigate conformational aspects of prion pathogenesis. The aptamers are 2′-fluoro-modified RNA produced by *in vitro* selection from a large, randomized library. One of these ligands (aptamer SAF-93) had more than 10-fold higher affinity for PrP^{Sc} than for recombinant PrP^{C} and inhibited the accumulation of PrP^{res} in near physiological cell-free conversion assay. To understand the molecular basis of these properties and to distinguish specific from nonspecific aptamer-PrP interactions, we studied deletion mutants of bovine PrP in denatured, α-helix-rich and β-sheet-rich forms. We provide evidence that, like scrapie-associated fibrils (SAF), the β-oligomer of PrP bound to SAF-93 with at least 10-fold higher affinity than did the α-form. This differential affinity could be explained by the existence of two binding sites within the PrP molecule. Site 1 lies within residues 23–110 in the unstructured N terminus and is a nonspecific RNA binding site found in all forms of PrP. The region between residue 90 and 110 forms a hinge region that is occluded in the α-rich form of PrP but becomes exposed in the denatured form of PrP. Site 2 lies in the region C-terminal of residue 110. This site is β-sheet conformation-specific and is not recognized by control RNAs. Taken together, these data provide for the first time a specific ligand for a disease conformation-associated site in a region of PrP critical for conformational conversion. This aptamer could provide tools for the further analysis of the processes of PrP misfolding during prion disease and leads for the development of diagnostic and therapeutic approaches to TSEs.

A simple observation that emerges from the examination of the structures of all mammalian recombinant PrPs[1] that have been solved so far in their α-helix-rich forms is that they have a highly positively charged N-terminal tail that is flexibly disordered and a stable globular C-terminal domain (1–10). It is becoming clear that these structural features must have some functional significance. Indeed, there is increasing evidence that PrP may accomplish its as yet unknown physiological function by allowing both the structured C-terminal domain and the unstructured N-terminal part to interact with a variety of ligands.

The C-terminal domain seems to interact with a protein X that is thought to feature in the conversion of PrP^{C} into PrP^{Sc} by acting like a molecular chaperone in facilitating the unfolding of PrP^{C} and its refolding into nascent PrP^{Sc} (11, 12). Protein X appears to bind to the side chains of residues 165–171 that form a loop and to residues on the surface of helix C that lie between the disulfide bond and the C terminus (12).

The unstructured N-terminal part of PrP can interact with a variety of molecules. Metal binding of PrP resides primarily in an octapeptide repeat motif between residues 53 and 93 (13). Although a more distal site has also been proposed (14), there seems to be a connection between metal-binding status and the conformation of PrP (15–17). Sulfated glycans interact with PrP (18) of which heparin and heparan sulfate have been shown to have three broad binding sites: residues 23–52, 53–93, and 110–123 (19). The binding of heparin and copper co-map to residues 53–93 and, interestingly, heparin binding seems to be enhanced by copper ions (19, 20). Large and small nucleic acids (21–24) also interact with PrP. It has been shown that human, ovine, and murine PrPs possess nucleic acid binding and chaperoning activities similar to retroviral nucleocapsid protein (25, 26), and these properties are associated with the unstructured N-terminal region of the protein (5, 10). Previously reported 2′-OH aptamers raised against recombinant hamster prion protein bound to a site between residues 23–52 within this nonspecific nucleic acid binding region (27). The physiological implications of the interactions between PrP and nucleic acid raise a number of questions that are still a matter of speculation (23–26,28).

All of the published studies in which interactions between PrP and nucleic acids have been demonstrated were done with the α-helix-rich form of PrP. To extend these studies we decided to isolate nucleic acids that had high affinity for an infectious, prion-containing material. We used purified, non-proteinase K-treated scrapie-associated fibrils (SAF) prepared from the 263K strain as a target during *in vitro* selection for apatmer. This SAF preparation is expected to include all variant PrP conformations and PK sensitivities associated with infectivity in this strain of prion, and should represent an appropriate target to investigate the capacity of PrP^{Sc} as well as other

* This work was supported by Biotechnology and Biological Sciences Research Council Grants 43/BS309665 and 43/BSD17731 (to W. S. J. with A. T. A. as the designated principal researcher). The costs of publication of this article were defrayed in part by the payment of page charges. This article must therefore be hereby marked "*advertisement*" in accordance with 18 U.S.C. Section 1734 solely to indicate this fact.

¶ Present address: VLA Lasswade, International Research Centre, Pentlands Science Park, Bush Loan, Penicuik, Midlothian EH26 OPZ, UK.

‖ To whom correspondence may be addressed. Tel.: 44-0-1865-275545; Fax: 44-0-1865-285756; E-mail: william.james@path.ox.ac.uk.

** To whom correspondence may be addressed. E-mail: abdou.tahiri-alaoui@path.ox.ac.uk.

[1] The abbreviations used are: PrPs, prion proteins; SAF, scrapie-associated fibrils; PVDF, polyvinylidene difluoride; TSE, transmissible spongiform encephalopathy.

```
SAF-93  ~~~~~~ CUAC GAACUCAUGA CACAAGGAUG CAAUCUCAUC CCGCCAGCCC ACCGU
SAF-126  ~~~GAUAUCA ACAUUAGGGC UCCUUGGGGA CCAGCGUCUC CUUGCAGCCC CGA
SAF-76  ~~ CCUGCUCC UCUAGCACCA UAUCCAAGCU ACAACUUCAC AACGACUCGG CC
SAF-82  ~ CUACGUUCC UUAUCCUCCC UUCAGGAACC UGUACACCAC AUUGCUGCCG AC
SAF-113  ~~~~~CCCUG GGUUUCGACC AGCACCUUGA CCGAUUCCAC AGCUCUGCGG GAGA
SAF-131  GCUGACCACC GCCAACGCAA CCUCCAAUGA CUUGGAUCAC CUAGACGAU~
```

FIG. 1. **Sequence alignment of isolated aptamers.** The random regions from six SAF-aptamer clones were aligned using Pileup from GCG, Wisconsin.

proteins that co-purify with it to retrieve high affinity aptamer ligands from a complex combinatorial RNA library.

We provide evidence that, like SAF, the β-oligomer of PrP bound to SAF-93 with at least 10-fold higher affinity than did the α-form. This differential affinity could be explained by the existence of two binding sites within the PrP molecule: Site 1 lies within residues 23–110 in the unstructured N terminus and is a nonspecific RNA binding site found in all forms of PrP. The region between residues 90 and 110 forms a hinge region that is occluded in the α-rich form of PrP but becomes exposed in the denatured form of PrP. Site 2 lies in the region C-terminal of residue 110. This site is β-sheet conformation-specific and is not recognized by control RNAs. Taken together, these data provide for the first time a specific ligand for a disease conformation-associated site in a region of PrP critical for conformational conversion. We also provide evidence that SAF-93 inhibits the accumulation of PrP^{res} in the cell-free conversion assay under near physiological conditions.

MATERIALS AND METHODS

In Vitro Selection—All oligonucleotides used in this study were described before (29). RNAs used for *in vitro* selection were produced by *in vitro* transcription with T7 RNA polymerase in presence of 2′-fluoro-modified pyrimidine nucleotide triphosphates (TriLink BioTechnologies, Inc., San Diego, CA), together with unmodified purine ribonucleotides in an optimized transcription buffer (30). The 2′-F-RNA transcripts were purified by electrophoresis on a 10% (w/v) denaturing polyacrylamide gel in TBE buffer. The pool of gel-purified 2′-F-RNA was heat denatured for 2 min at 95 °C in deionized and filter-sterilized water, refolded for 10 min at room temperature in HMKN buffer (20 mM Hepes pH 7.2, 10 mM $MgCl_2$, and 50 mM KCl, 100 mM NaCl), before being used for the selection process. The refolded 2′-F-RNA pool (5 nmol) was incubated with SAF purified from approximately one-half of a hamster brain, prepared as described below. Before each round of selection an aliquot of SAF was sonicated in a cup-horn probe with three pulses of 1 min each with an amplitude set at 40 and an output of 20 watts. The binding reaction was done at room temperature in HMKN buffer for 4 h. After partitioning the binding reaction was centrifuged for 1 h at 25,000 $\times$ *g* at 10 °C. The amount of unbound 2′-F-RNA in this first supernatant was stored at −20 °C. In order to remove nonspecifically bound 2′-F-RNA, the pellet containing 2′-F-RNA-SAF complex was washed three times with 100 μl of HMKN buffer. The supernatants from each wash were pooled with the first supernatant and the amount of unbound 2′-F-RNA determined by spectrophotometer (GeneQuant, Amersham Biosciences). The bound RNA was converted to cDNA by reverse transcription with *Thermus thermophilus* (Tth) DNA polymerase at 70 °C for 20 min followed by 15 cycles of PCR amplification following the protocol provided by the supplier (Promega). The resulting PCR products were used as template for *in vitro* transcription to produce RNA for the next round of selection. The pool of RNA from round 7 was converted into DNA and cloned into pUC18 (29).

Preparation of Scrapie-associated Fibrils for Selection—SAF were prepared from the brains of hamsters that were infected with the 263K strain of scrapie (31). SAF were prepared without proteinase K treatment as described by Hope *et al.* (32). This preparation should include all variant PrP conformations and PK sensitivities associated with infectivity in this strain of prion. The final pellet (P285) was washed several times in water to remove traces of sarcosinate, before being resuspended in HMKN buffer pH 7.2 containing 0.02% (w/v) azide and stored at +4 °C.

Protein Preparation and Refolding—Truncated bovine PrPs, corresponding to residues 90–230 and 110–230 (human numbering) with His-tag at the N terminus were cloned, expressed, and purified as described before (33). Full-length bovine PrP corresponding to residues 23–230 without any tag was obtained by PCR amplification of genomic DNA and inserted as *Bgl*II-*Eco*RI restriction fragments into expression plasmid pMG939 (34) and amplified in *Escherichia coli* K12 1B392/pACYRIL, which overexpresses rare arginine, isoleucine, and leucine tRNAs. Cultures were grown to saturation in Terrific Broth containing 100 μg/ml ampicillin and 15 μg/ml chloramphenicol at 30 °C then diluted 400-fold. In late-log phase, expression of PrP was induced by raising the temperature from 30 °C to 45 °C for 10 min, followed by incubation at 42 °C for 5 h. The cells were then harvested by centrifugation at 10 000 $\times$ *g* for 15 min. The pellet was resuspended in ice-cold lysis buffer (50 mM Tris-HCl, pH 8.0, 100 mM NaCl, 2 mM phenylmethylsulfonyl fluoride, 10 μg/ml lysozyme, 10 μg/ml DNase I, 1 mg/ml sodium deoxycholate) and incubated for 30 min at 37 °C. The solution was then centrifuged at 10,000 $\times$ *g* for 30 min, and the supernatant discarded. The pellet was washed twice by resuspension in lysis buffer with centrifugation at 10,000 $\times$ *g* for 10 min between each wash. Proteins in the pellet were dissolved by suspending it in buffer A (100 mM sodium phosphate, 10 mM Tris, pH 8.0, 8 M urea, and 10 mM 2-mercapthoethanol) and incubating for 30 min with gentle mixing. Cell debris and insoluble material were removed by centrifugation at 15,000 $\times$ *g* for 15 min. The supernatant was loaded onto a Ni-NTA-Sepharose column (Qiagen Ltd.) pre-equilibrated with buffer A. After washing the column with the same buffer, bound proteins were eluted with buffer B (100 mM sodium phosphate, 10 mM Tris, pH 4.5, 8 M urea, and 10 mM 2-mercaptoethanol). For further purification the eluate from the column was diluted 1:2 with buffer C (50 mM Hepes pH 8.0, 8 M urea, and 10 mM 2-mercapthoethanol) and loaded onto a cation exchange chromatography column, SP-Sepharose (Amersham Biosciences). Recombinant PrP was eluted with buffer C supplemented with 1.5 M NaCl. Eluted fractions of recombinant PrP were pooled, and disulfide bonds were oxidized by stirring overnight in a 2:1 molar excess of $CuCl_2$. After oxidation, the protein solution was dialyzed against 50 mM sodium acetate, pH 5.5, 1 mM EDTA, with several changes of buffer. Finally, the recombinant PrP was applied onto a size-exclusion chromatography column (Superdex 75 HR 10/30, Amersham Biosciences) equilibrated and eluted with 50 mM sodium acetate, pH 5.5.

The purified PrPs were refolded into native α-helical conformation or β-oligomeric isoform following the protocol described by Baskakov *et al.* (35). Size exclusion chromatography were performed at room temperature with a flow rate of 1 ml/min using either a TSK-3000 or a BIOSEP-S3000 HPLC column (300 $\times$ 7.8 mm) from Phenomenex, equilibrated in 20 mM sodium acetate, pH 3.7, 0.2 M NaCl, and 1 M urea. The main peak corresponding to monomeric α-helical rich form or β-oligomer isoform of PrP was manually collected and assessed by CD. The protein concentration was determined spectrophotometrically using the molar extinction coefficient (ϵ_{280}) of 19 890 M^{-1} cm^{-1} for $boPrP^{90-230}$, and of 62,280 M^{-1} cm^{-1} for $boPrP^{23-230}$. The PrP peptide spanning the region 106–126 was synthesized, purified, and analyzed as described before (36).

Circular Dichroism—CD spectra were recorded with a Jasco J-720 CD spectrometer using the following parameters: scanning at 200 nm/min, bandwidth of 2 nm, data spacing of 0.1 nm and using a 0.05- or 0.02-cm cuvette. Twenty individual scans were averaged, and the background spectra were subtracted.

Affinity of Monoclonal Aptamer for SAF—All RNAs used in this study were ^{32}P-labeled at the 5′-end as described before (29). Scrapie-associated fibrils from 263K strain of scrapie were prepared as described above. The final pellet from one hamster brain was resuspended in 200 μl of HMKN buffer and submitted to ultrasonication. For homologous competition, 2 μl of either proteinase K-treated or -untreated SAF, were incubated with 7000 cpm of ^{32}P-labeled monoclonal SAF-93 in HMKN buffer containing 1 μg of tRNA and the mixture incubated for 1 h at room temperature. Cold homologous aptamer was added to each tube in 2-fold increasing concentrations from 0.25 to 8192 nM and incubated for 1 h. The displaced hot aptamer in each tube was separated from the remaining bound aptamer by centrifugation at 25,000 $\times$ *g* and 10 °C for 20 min. The resulting pellet was resuspended in water, and the amount of radiolabeled aptamer measured by Cerenkov counting. Each competition experiment was done in triplicate, and the data were analyzed by GraphPad PRISM.

Affinities of Monoclonal Aptamer for PrPs—Radiolabeled SAF-93 or control aptamer 19 (10,000 cpm Cerenkov) were heat-denatured in

water for 1 min at 95 °C, cool to room temperature for 3 min before allowing it to refold in presence of 20 mM sodium acetate pH 5.2, 150 mM NaCl, 50 mM KCl, and 5 mM $MgCl_2$ for 10 min at room temperature. The refolded aptamer was then mixed with a range of increasing concentrations of PrP in various forms and lengths in presence of 1 M urea and 1 μg of tRNA as nonspecific competitor in a total volume of 20 μl. The binding reactions were incubated for 2 h at room temperature. In order to separate the free aptamer from PrP-aptamer complex we have used Strataclean™ resin (Stratagene) that has the property to pull-down proteins and RNA-protein complex by simple and quick centrifugation. Three μl of Strataclean™ resin (Stratagene) was added to the binding reaction, and the mixture was vortexed and incubated for 1 min at room temperature before spinning in a benchtop centrifuge at top speed for 1 min. The resulting supernatant was transferred to a fresh tube, and the pellet washed with 20 μl of binding buffer without tRNA. The supernatant from the washed pellet was added to the previous supernatant, this supernatant formed the unbound aptamer. The complex aptamer-PrP remaining in the pellet was resuspended in 20 μl of binding buffer. The amount of radioactivity in both the supernatant, and the pellet was measured by Cerenkov counting. The binding data were analyzed by GraphPad Prism using a non-linear regression curve fitting and one site binding hyperbola equation: Fraction bound = $(B_{max} \times [PrP])/K_d + [PrP]$.

Slot Blots—We have used Bio-Dot® SF microfiltration apparatus and PVDF membrane (0.2-μm pore size) from BioRad assembled following the manufacturer's instructions. 90 pmol of PrPs in various forms and lengths were applied by vacuum onto the PVDF membrane that was previously equilibrated in 20 mM sodium acetate buffer, pH 4.4. The PVDF membrane containing PrPs was then incubated for 1 h in 15 ml of blocking solution containing 5× Denhardt's solution in HMNK buffer pH 7.2 and 20 μg/ml tRNA at room temperature. The blocking solution was replaced with a fresh one and supplemented with 400,000 cpm radiolabeled and refolded SAF-93 or control aptamer 19 and allowed to incubate for 2 h or overnight at 25 °C inside a hybridization oven under constant rolling. The membrane was then washed twice with 15 ml of HMNK buffer pH 7.2, wrapped inside a saran film and exposed to Storage phosphor screen for at least 2 h followed by scanning with the Storm imaging system and the autoradiographs analyzed with ImageQuant software from Molecular Dynamics.

SDS-PAGE and Western Blots—PrP proteins were separated under denaturing and reducing conditions on SDS-PAGE (37) using 18% polyacrylamide precast Novex gels (Invitrogen). After electrophoresis the gel was blotted (38) onto PVDF membrane and probed with either mAb 6H4 (Prionics) or mAb FH11 (TSE Resource center, IAH, Compton, UK) followed by a secondary antibody conjugated to alkaline phosphatase and detected with ECF substrate (Amersham Biosciences) using the chemiluminescent mode on the Storm imaging system from Molecular Dynamics. The detection with radiolabeled aptamers was performed as described under "Slot Blot."

Cell-free Conversion Assay—The cell-free conversion assay without guanidinium chloride was as described by Kirby *et al.* (39) and based on that used by Horiuchi and Caughey (40). Briefly PrP^{Sc} was sonicated and ~1 μg incubated with 200 ng of [^{35}S]shaPrP in conversion buffer (50 mM citrate, pH 6.5, 50 mM KCl, 10 mM $MgCl_2$, 100 mM NaCl, 0.1% (v/v) Nonidet P-40) with or without SAF-93 or control RNA, for 24 h at 37 °C in a 20-μl volume reaction. One-twentieth of the reaction was removed for analysis without proteinase K treatment, and the remaining was treated with 60 μg/ml of proteinase K for 1 h at 37 °C. Proteinase K digestion was stopped by addition of Pefabloc to 1 mM. All samples were precipitated with 20 μg of bovine serum albumin and 4 volumes of ice-cold methanol at −20 °C. The resulting pellet was boiled for 10 min in SDS-sample buffer and analyzed by 15% SDS-PAGE, fixed, dried, and exposed to film. Autoradiographs were quantified using Phoretix Gel Analysis software.

RESULTS

Isolation of PrP-specific 2′-F-RNA Aptamers—A DNA library comprising a 49 nucleotide randomized region was synthesized. In theory, this library could comprise $4^{49} = 8 \times 10^{28}$ distinct sequences although in practice, only ~10^{14} of these are sampled during the selection process (41). The library was transcribed to produce 2′-F-pyrimidine-substituted RNA and subjected to repeated cycles of *in vitro* selection for transcripts that bound to insoluble non-PK-treated PrP^{Sc} fibrils isolated from the brains of 263K scrapie-infected hamsters. PrP-binding 2′-F-substituted nucleic acids became a significant fraction of the population by selection round 3, and the pool from round 7 was cloned as cDNA.

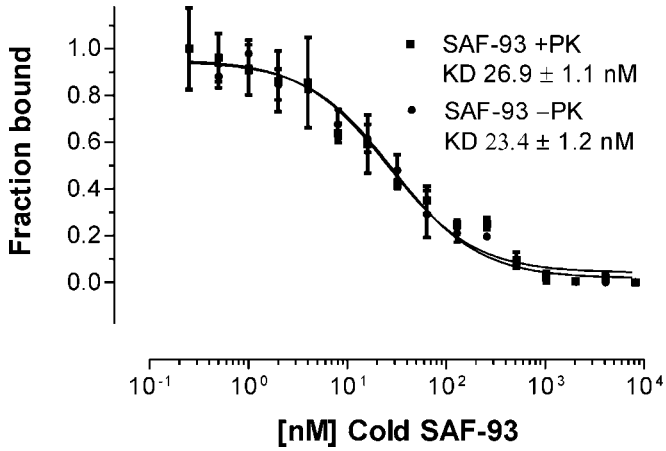

FIG. 2. **Affinity of aptamer SAF-93 for proteinase K-treated and untreated scrapie-associated fibrils.** Unlabeled SAF-93 was used as a competitor of the formation of complex between ^{32}P-end-labeled SAF-93 and SAF. The normalized data were fitted to the equation: Fraction bound = ([Hot93])/([Hot93] + [Cold93] + K_d) using non-linear curve fitting with GraphPad Prism software.

The sequences of the clones encoding ligands for PrP show that they probably derived from distinct members of the initial library (see Fig. 1). Some stretches of weak sequence homology between the six clones might reflect some convergence of structural features. In this study we present the data obtained from investigating the interaction between SAF-93 and PrP protein in various lengths and conformations.

Affinities of Aptamer for PrP Forms—The first step toward the characterization of the selected monoclonal 2′-F-SAF-aptamers was to determine the strength of their binding to SAF used as a target during the *in vitro* selection. We have used a homologous competition binding assay in which we have measured the binding of a single concentration of ^{32}P-end-labeled SAF-93 to SAF preparation in presence of an increasing concentration of the same unlabeled aptamer (Fig. 2). The fitting of homlogous competition data to a one site binding model (GraphPad Prism Software, Inc.) gave an estimated K_d of 23.4 ± 1.2 nM without proteinase K (PK)-treatment of SAF and a K_d of 26.9 ± 1.1 nM against PK-treated SAF. These data indicated that the aptamer binding site lay in the PK-resistant core of disease isoform PrP, comprising residues 90–230.

The biochemical and biophysical properties associated with the SAF material made it difficult to perform routine investigations in order to gain better understanding of the interaction between our aptamer and the disease-associated form of PrP. Therefore we decided to use purified bacterially-expressed recombinant bovine PrP of various lengths that had been refolded into α-helical conformation or β-oligomer form with an intact disulfide bridge as described by Baskakov *et al.* (35). The α-form and β-form (Fig. 3*A*) of bovine PrP eluted from the SEC with retention times very similar to those published for mouse PrP^{89-231} (35, 42). The peaks that eluted at 7.19 and 9.06 min were collected and analyzed by CD (Fig. 3*B*) and found indeed to correspond to β- and α-form of PrP^{90-230}, respectively. Similar results were obtained with the full-length PrP^{23-230} (data not shown).

We used the forms of recombinant bovine PrP described above in an equilibrium binding assay with radiolabeled SAF-93 in parallel with a radiolabeled control aptamer SA-19 that was isolated against streptavidin (29) in order to determine the equilibrium binding constant of the interactions (Fig. 4). The binding affinity of SAF-93 for the truncated β-PrP^{90-230}

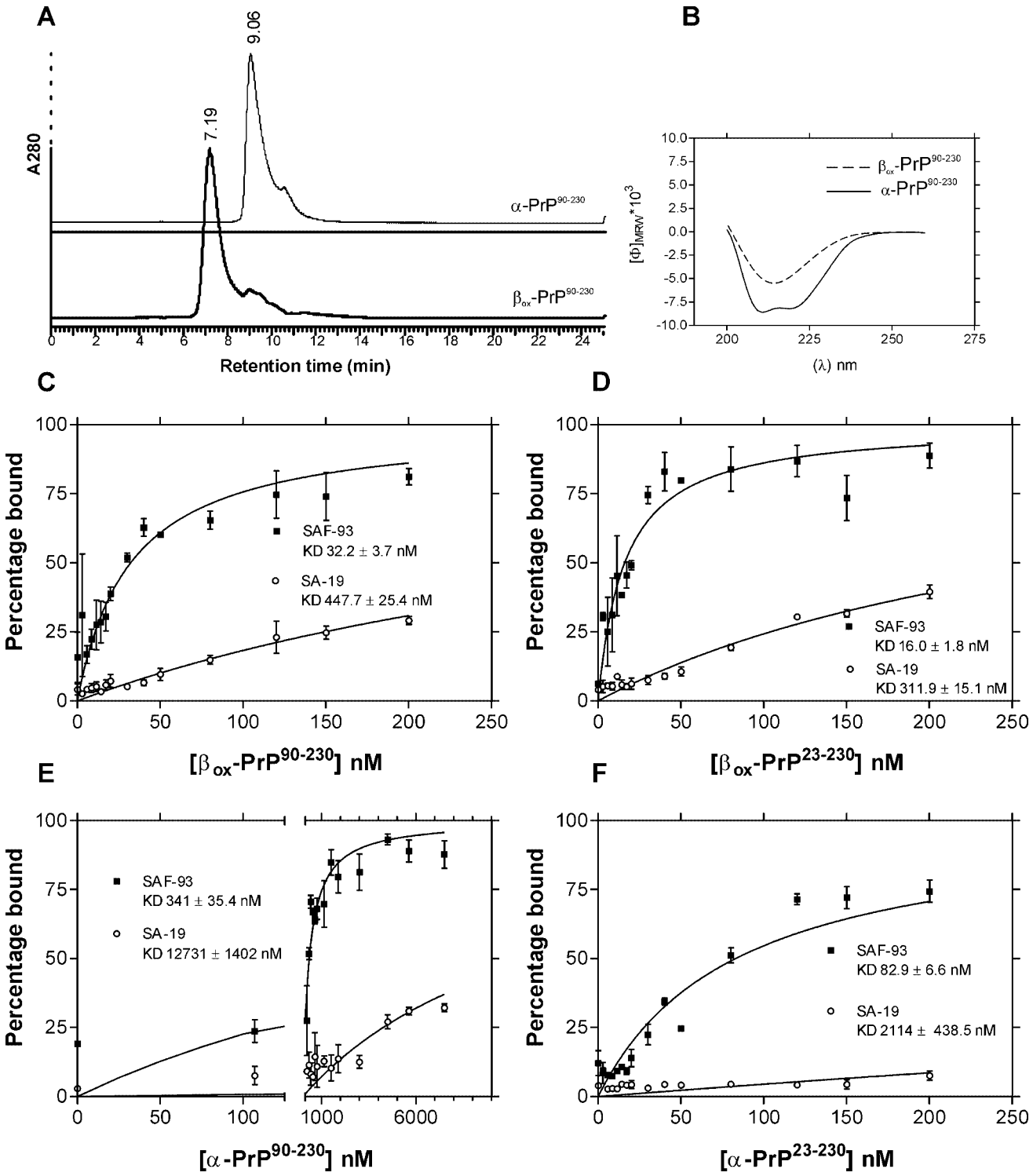

FIG. 3. **Refolding of recombinant bovine PrPs and affinity measurment.** *A*, SEC profile of recombinant PrPs that were refolded into either α-form (*thin line*) or $\beta_{oxidized}$-form (*bold line*). *B*, far UV CD spectra of the main peaks collected from SEC. The CD spectra were recorded in 20 mM sodium acetate, pH 3.7 containing 200 mM NaCl and 1 M urea, and confirmed the α-helix (*continuous line*) and the β-sheet (*short-dashed line*) conformations of PrP^{90-230}. The protein concentration was 4.3 and 6.8 μM for α- and β-forms, respectively. *C–F*, aptamer SAF-93 (*filled squares*) and aptamer SA-19 (*open circles*, control) were 5′-end-labeled to high specific activity and mixed with varying concentrations of $\beta_{oxidized}$-PrP^{90-230}, $\beta_{oxidized}$-PrP^{23-230}, α-PrP^{90-230}, and α-PrP^{23-230}, respectively. PrP-bound and unbound aptamer were partitioned using Strataclean resin and the fraction bound determined as described. Data were fitted to a hyperbolic function by non-linear curve fitting method of GraphPad PRISM. The result of the fitting is represented by *solid line*. The x-axis in *panel F* has been split and rescaled to better highlight the differences in affinities between α- and β-form PrP.

and full-length β-PrP^{23-230} was found to be 32.2 nM (Fig. 3*C*) and 16.0 nM (Fig. 3*D*), respectively. Significantly, these affinities were close to those determined for the PK-treated and -untreated SAF (see above), indicating that SAF-93 recognized a binding site that was common between SAF and *in vitro* refolded β-form PrPs and that the aptatope was conserved between these two species.

When the affinity of SAF-93 for α-PrP^{90-230} (Fig. 3*E*) and α-PrP^{23-230} (Fig. 3*F*) was measured, the affinity was found to be 10- and 5-fold less than that measured for the β-form

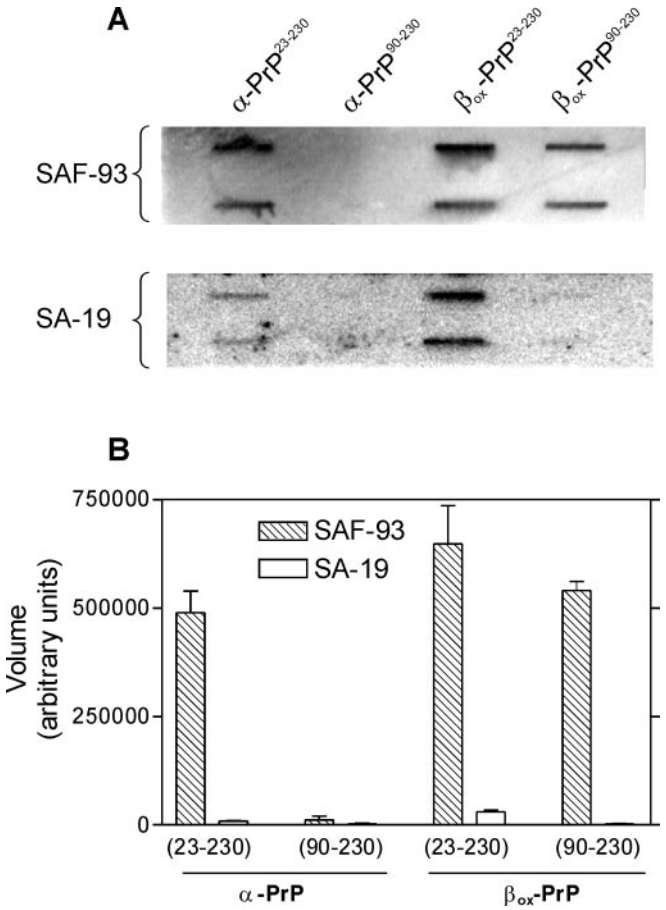

FIG. 4. **Binding of SAF-93 to folded PrP derivatives.** *A*, 90 pmol of α-PrP$^{23-230}$, α-PrP$^{90-230}$, $\beta_{oxidized}$-PrP$^{23-230}$, and $\beta_{oxidized}$-PrP$^{90-230}$ were applied in duplicate onto PVDF membrane using the Slot blot apparatus (Bio-Rad) and the proteins detected with either [^{32}P]SAF-93 or with [^{32}P]SA-19 as control aptamer. The intensity of the displayed digital picture had to be increased in order to make the bands visible. However, the quantitation analysis has been done on the original unmodified picture. The bands were then detected by Storage Phosphor technology. *B*, the bands were analyzed with ImageQuant software.

PrP$^{90-230}$ and β-form PrP$^{23-230}$, respectively. When compared with SAF-93, the control aptamer SA-19 has an affinity that was at least 10-fold lower for both conformations and lengths of PrPs (Fig. 3, *C–F*).

As a complementary approach, the binding of SAF-93 to the same PrPs was assayed under native conditions by slot blotting. The results revealed that preserving the conformation of the aptamer binding site was essential for maintaining the discriminatory power between α- and β-form PrPs, and that was most marked for PrP$^{90-230}$ (Fig. 4, *A* and *B*). SAF-93 could only bind to PrP$^{90-230}$ in its β-form, while the binding to α-form was virtually abolished (Fig. 4, *A* and *B*). Under these conditions, SAF-93 bound equally well to α- and β-form PrP$^{23-230}$ (Fig. 4, *A* and *B*). Both approaches led to qualitatively similar conclusions. First, the aptamer binding site was occluded in α-PrP$^{90-230}$ and only became accessible to the aptamer in β-PrP$^{90-230}$. Second, the conformation-specific binding site for SAF-93 resided downstream of residue 90. Third, the binding site for SAF-93 in the unstructured N-terminal segment upstream of residue 90 was conformationally nonspecific and could represent a region of PrP with high nucleic acid binding propensity.

Mapping the Binding Site of SAF-93 on PrP—Since the PK treatment of SAF and the truncation of recombinant bovine PrP did not affect the binding properties of the aptamer, it was clear that a binding site resided within the PK resistant core of PrP (residues 90–230). In attempting to define the binding site more precisely, we were helped by the fortuitous appearance of a defined degradation product of PrP in Western blotting experiments (see Fig. 5).

Coomassie Blue staining of the gel (Fig. 5*A*) showed one major band for α-PrP$^{23-230}$ with the expected molecular mass of 23.6 kDa, whereas the α-PrP$^{90-230}$ revealed two bands of approximately equal intensities: a band with a molecular mass of 15.9 kDa as one would expect from the bovine PrP residues 90–230, and another band with a lower molecular mass (Fig. 5*A*). Mass spectrometry analysis of the protein sample in solution revealed that it contained both PrP$^{90-233}$ and PrP$^{110-230}$ (data not shown). In the absence of other signals we concluded with 99% confidence that the fragment 110–230 was what caused the second band on the gel. Similar proteolysis digestion has been reported for recombinant murine prion protein (20, 43). When the blot derived from this gel was probed with [^{32}P]SAF-93 (Fig. 5*B*), two clear bands were detected that corresponded to PrP$^{23-230}$ and PrP$^{90-230}$. The probing with ^{32}P-control aptamer, SA-19, revealed a similar detection pattern, but with significantly lower intensities than those obtained with SAF-93 (see Fig. 5*C*). In fact, the intensity of the displayed digital picture had to be substantially increased in order to make the two bands visible. The identity of the two bands detected with SAF-93 was further confirmed by probing similar blots with mAb 6H4 (Fig. 5*D*) and as expected, PrP$^{90-230}$ was not detected by mAb FH11 (Fig. 5*E*). Most significantly, the band that corresponded to PrP$^{110-230}$ was not detected by SAF-aptamer 93, indicating that an essential part of the aptamer binding site spanned residues 90–110. In order to further characterize the interaction between SAF-93 and PrP$^{110-230}$, the latter was cloned, expressed, purified, and characterized by SDS-PAGE (Fig. 6*A*). We confirmed that under denaturing conditions and using North-Western blot assay SAF-93 did not bind to PrP$^{110-230}$ (Fig. 6*B*) nor did control aptamer SA-19 (Fig. 6*C*), whereas the reactivity of this protein toward mAb 6H4 was maintained as expected (Fig. 6*D*). Importantly, when PrP$^{110-230}$ was refolded into β-form as before, we found that the binding affinity toward SAF-93 was restored to values (Fig. 6*E*) very close to those calculated for β-PrP$^{23-230}$ and β-PrP$^{90-230}$ (see Fig. 3, *C* and *D* for comparison). When PrP$^{110-230}$ was folded into the α-form its interaction with SAF-93 was abolished (Fig. 6*F*). The control aptamer SA-19 bound only weakly to β-PrP$^{110-230}$ (Fig. 6*E*) and not at all to α-PrP$^{110-230}$ (Fig. 6*F*). These data provided strong evidence for the existence of a conformation-specific SAF-93 binding site downstream of residue 110. This conformation-specific aptatope is not recognized by the aptamer when the PrP$^{110-230}$ is denatured or folded into the α-form.

Numerous studies have indicated that the region 106–126, just upstream of the first β-sheet, is a conformationally flexible part of the protein (36, 44, 45) and is neurotoxic (46–50). Because of the overlap between this "neurotoxic peptide" region and that defined as containing an SAF-93 binding site, we decided to test whether SAF-93 could bind to peptide PrP$^{106-126}$. By adjusting the buffer conditions, we could fold this peptide into a β-form, or retain it in a random coil conformation (see Fig. 7*A*). The affinity of SAF-93 was found to be very similar between the unstructured (Fig. 7*B*) and the β-form (Fig. 7*C*) of PrP$^{106-126}$, in the order of 400 nM, which is very close to the affinity value measured for α-PrP$^{90-230}$ determined above. However, as the affinity for β-forms PrP had been found to be in the 20–30-nM range (see above), this indicates that the region 106–126 might contain only part of the aptamer binding site or that the folding of the peptide into β-form did not

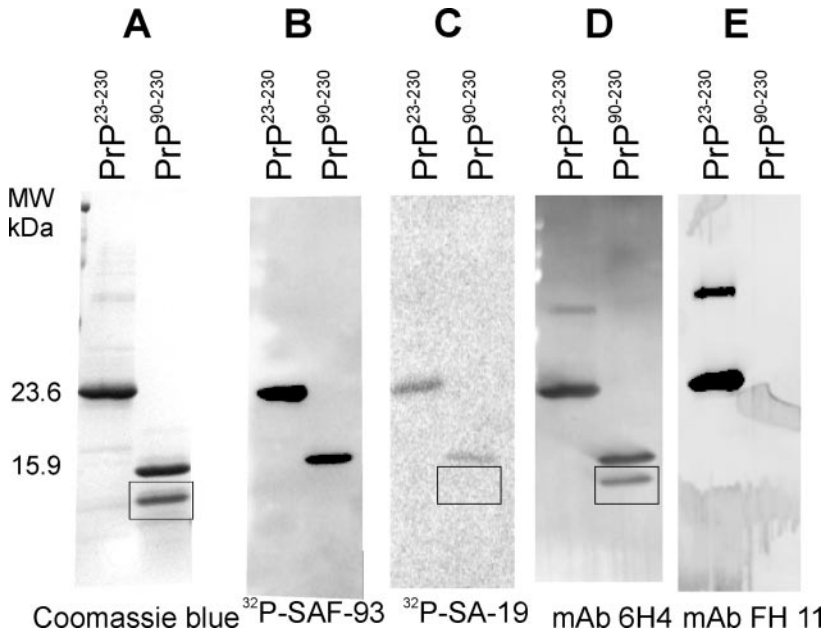

FIG. 5. **Binding of SAF-93 to denatured PrP derivatives.** *A–E*, recombinant bovine PrPs were analyzed on 18% SDS-PAGE and then either stained with Coomassie Blue, or blotted onto PVDF membrane and probed with [^{32}P]SAF-93, [^{32}P]SA-19 (control aptamer), mAb 6H4, or mAb FH11, respectively. The band framed in *panel A,* is a proteolysis fragment that was confirmed by mass spectrometry to correspond to residues 110–230.

faithfully represent the folding of this region in the context of PrP^{Sc}.

Inhibition of Cell-free Conversion of PrP by Aptamer—The preferential binding of SAF-93 to the disease-related β-form PrP prompted us to investigate the capacity of this artificial ligand to interfere with the conformational switch that leads to the accumulation of PrP^{res}. We have used the cell-free conversion system under near-physiological conditions in order to give more biological relevance to the assay as a model for conversion. In this study, recombinant hamster PrP was radiolabeled during expression, purified from bacteria and refolded *in vitro* (39). [^{35}S]ShaPrP was incubated in the presence of unlabeled PrP^{Sc} isolated from 263K scrapie-infected hamster brains, with or without control RNA or with increasing concentrations of SAF-93 in a guanidine-free conversion buffer at 37 °C for 24 h. Following proteinase K digestion, SDS-PAGE analysis and autoradiography (Fig. 8*A*), the intensity of the band at ~17.4 kDa, representing the PK-resistant core of [^{35}S]$ShaPrP^{res}$, decreased with increasing amounts of SAF-93. Even at the highest concentration, the unselected 2′-F-RNA library produced no significant inhibition of conversion (Fig. 8*A*). Similar results were obtained when the control SA-19 aptamer (29) was used instead of the unselected RNA library (data not shown). These data showed that there was a specific SAF-93-dependent inhibition of the accumulation of PrP^{res} protein. The average IC_{50} titer was estimated from the dose response graph in Fig. 8*B* and found to be around 40 nM for SAF-93.

DISCUSSION

Here we describe the isolation of novel nucleic acid ligands or aptamers for PrP, the key protein in the pathogenesis and the transmission of vCJD, BSE, and other TSEs. Because of the high propensity of recombinant PrP to interact with nucleic acid via its unstructured N-terminal domain, it was of paramount importance to discriminate between specific and nonspecific interactions. The first indication of specificity of aptamer SAF-93 came from the homologous competition assay. The fact that binding affinity was not affected by proteinase K treatment of SAF material, suggested that the aptatope lay in the PK-resistant core of PrP, comprising the 141 amino acids in the C-terminal portion of the protein, from residue 90 to 230. Moreover, the binding affinity measured for β-oligomer PrP spanning residues 90–230 was very close to that of SAF material that has been treated with proteinase K. These suggest conformational similarities between SAF and β-oligomer PrP^{90-230}. In the light of the recently published data by Baskakov *et al.* (35), it is very important to stress at this point that these structural similarities might be just subtle enough to account for the existence of a common β-sheet rich aptatope between SAF material and β-oligomer PrP, even though the latter is not considered to be on the kinetic pathway for amyloid formation and cannot be regarded as a substructure of the fibrillar form (35). Because PrP^{Sc} and PrP^{C} both maintain the disulfide bridge (51) we believe that it was more relevant to use the non-reduced PrP to generate the β-oligomer form. However, we found that SAF-93 maintained the same binding affinity against β-form PrP with no disulfide bridge (33).[2] The simple explanation for this is that the absence of the disulfide bridge does not affect local folding into a β-sheet of the region downstream of residue 90 where SAF-93 aptatope occurs. In agreement with this explanation is the fact that all structures of recPrPs showed that the disulfide bridge is located between helix B and helix C, which seemed to maintain their global conformation in the plausible models for the structure of PrP^{Sc} (52).

The molecular basis for the preferential recognition of β-oligomer PrP by SAF-93 is still unclear, but our data reinforce and extend previous reports that RNA interactions with proteins are generally more favorable with β-sheet than α-helix (53). We were fully aware of the fact that the analysis of the binding data with an equation that governed one binding site might not reflect the true complexity of the interaction between aptamers and PrP. However, we have analyzed the binding data between SAF-93 and β-PrP^{23-230} with an equation that described the existence of two independent binding sites. We found an affinity value for the nonspecific site (1) of 8 μM while the conformation-specific site (2) had an affinity value of 16 nM; a value that remained identical to that obtained by fitting the data to one binding site equation. This reinforces the idea that the binding of SAF-93 to β-form PrPs 23–230, 90–230, and 110–230 could be accounted for by the existence of only the conformation-specific and low affinity site (2).

[2] A. Rhie, N. Sayer, P. Disterer, W. James, and A. Tahiri-Alaoui, unpublished data.

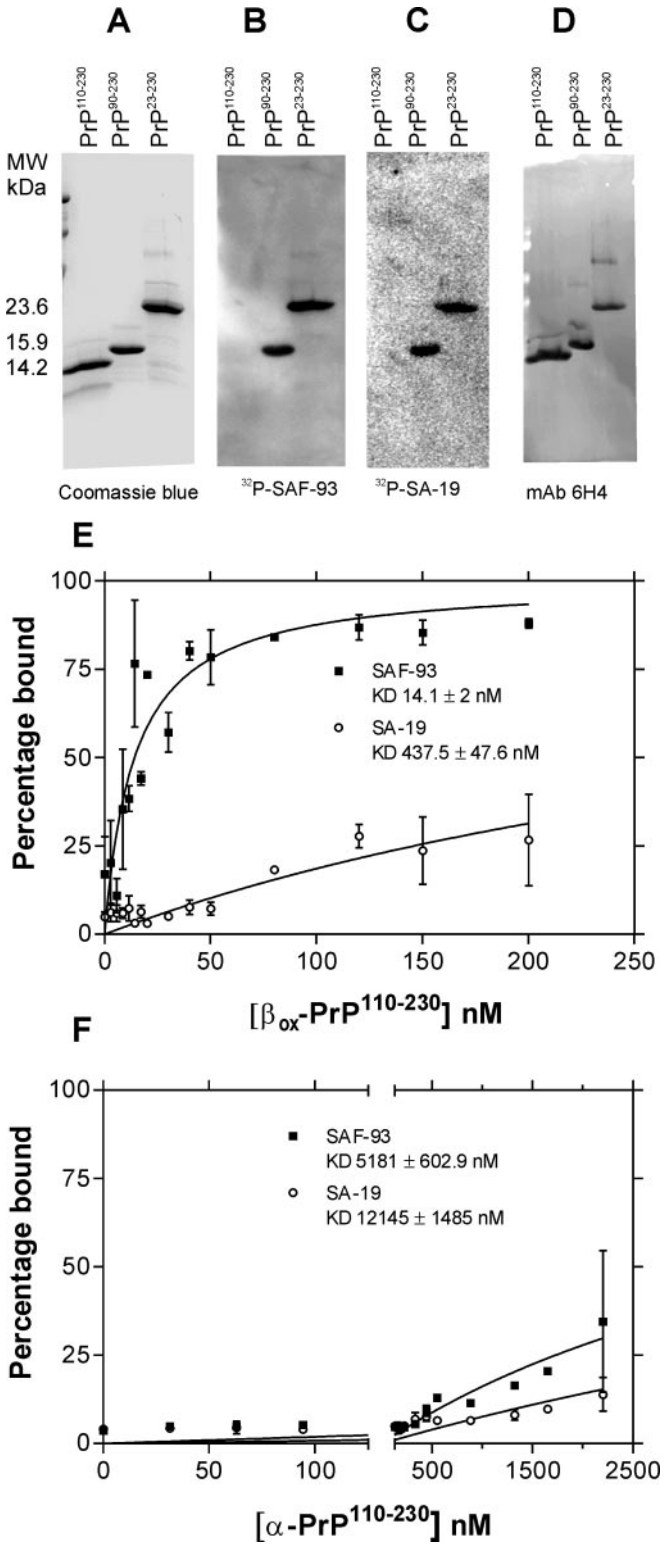

FIG. 6. **Binding affinity of SAF-93 to PrP$^{110-230}$.** *A–D*, a derivative of recombinant bovine PrP corresponding to residues 110–230 was characterized as described in Fig. 5. PrP$^{23-230}$ and PrP$^{90-230}$ were analyzed in parallel for direct comparison. *E* and *F*, the fraction of [^{32}P]SAF-93 (*filled squares*) or ^{32}P-SA-19 (*open circles*, control aptamer) bound by increasing concentration of $\beta_{oxidized}$-PrP$^{110-230}$ and α-PrP$^{110-230}$, respectively were determined as before. Data were fitted to a hyperbolic function by non-linear curve fitting method of GraphPad PRISM. The result of the fitting is represented by *solid line*. The x-axis in *panel F* has been split and rescaled to better highlight the differences in affinities between α- and β-form PrP.

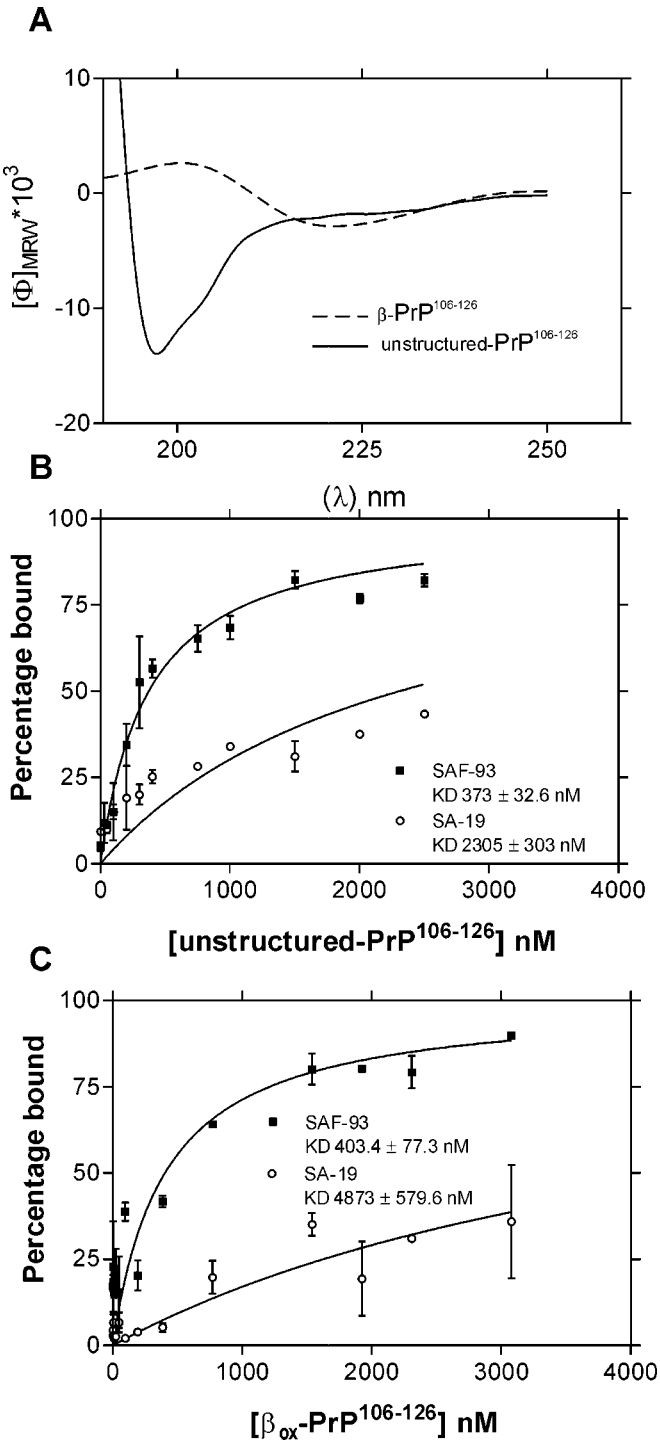

FIG. 7. **Binding affinity to unstructured and β-form PrP$^{106-126}$.** *A*, far UV CD spectra of PrP peptide 106–126 refolded into β-form (*short-dashed line*) after incubation for at least 2 h in 10 mM potassium phosphate pH 8.0 and mixing it with 20 mM sodium acetate, pH 4.8, containing 100 mM NaCl, 50 mM KCl and 10 mM $MgCl_2$; the final pH was 5.4. These buffer conditions were compatible with those used to determine the binding affinity as well as to obtain a peptide population that is highly populated with a β-form. The unstructured form of PrP$^{106-126}$ (*continuous line*) was simply obtained by incubating the peptide in 20 mM sodium acetate, pH 5.4, containing 100 mM NaCl, 50 mM KCl, and 10 mM $MgCl_2$. The peptide concentration was 140 μM. *B* and *C*, [^{32}P]SAF-93 (*filled squares*) or [^{32}P]SA-19 (*open circles*, control aptamer) bound to increasing concentration of unstructured-PrP$^{106-126}$, β-PrP$^{106-126}$, respectively, were determined as before. Data were fitted to a hyperbolic function by non-linear curve fitting method of GraphPad PRISM. The result of the fitting is represented by *solid line*.

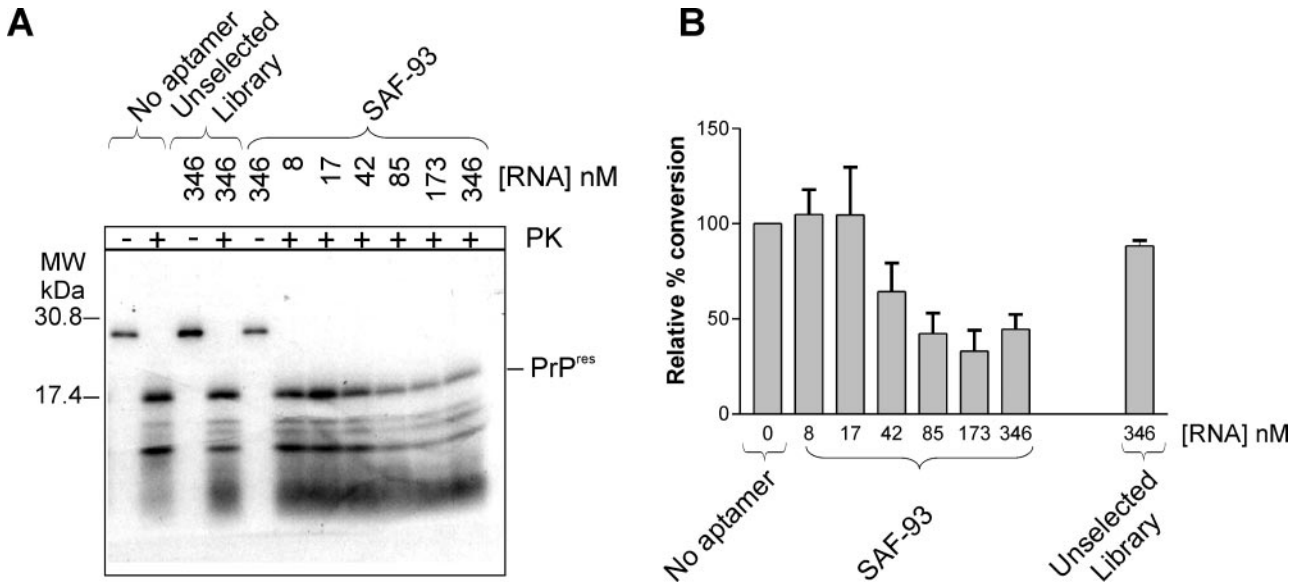

FIG. 8. **Inhibition of conversion of PrP^{sen} to PrP^{res} by SAF-93 in a cell-free assay.** *A*, 1 μg of SAF were mixed with [^{35}S]ShaPrP^{sen} in a 20-μl reaction mixture with or without unselected RNA pool and increasing concentrations of SAF-93. After 24 h of incubation at 37 °C, aliquots were analyzed by SDS-PAGE either with or without proteinase K digestion. The gels were then dried and imaged by autoradiography. *B*, results from four independent experiments are plotted as the percentage of [^{35}S]PrP^{res} generated in the cell-free conversion assay in the presence of SAF-93 or the unselected RNA pool relative to the amount of PrP^{res} generated in the absence of unselected RNA pool or SAF-93 as determined by densitometry.

The data from the mapping of the aptamer binding site onto PrP conformations provided a basis to explain the aptamer-dependent inhibition effect on the conversion of [^{35}S]ShaPrP^{sen} to PrP^{res}. Although the molecular mechanisms of this conversion are as yet to be elucidated, direct interaction between PrP^{Sc} and [^{35}S]ShaPrP^{sen} is critically important. Two non-exclusive mechanisms could explain the inhibition of the conversion by aptamer. First, the aptamer could bind directly to the PrP^{Sc} used as a template for conversion, therefore preventing any direct and critical contact between [^{35}S]ShaPrP^{sen} and PrP^{Sc}. Second, and by virtue of its high affinity to the β-rich PrP, the aptamer might bind to any escaped *de novo* formed β-rich PrP and thereby stall the conversion.

Antibody mapping has indicated sites of interaction between PrP^{sen} and PrP^{res}. One or more of these areas were adjacent to the C terminus in the three-dimensional structure of PrP^{sen} (40, 54). One such surface contains residues 119–138 and others contain residues 165–174 and 206–223. Antibodies that bind to these areas are capable of interfering with PrP^{res} accumulation (40). The inability of antibodies recognizing residues 90–104 and 106–115 to inhibit PrP^{res} formation has been attributed to conformational rearrangements occurring during the process of conversion that might induce the antibody to dissociate (40). Indeed, many biochemical and spectroscopic studies concord to suggest that the region 90–124 undergoes a major conformational change during the formation of PrP^{res} (2, 5, 36) and (55–57). Intriguingly, the site we suggest for SAF-93 binding lies in a region defined recently by us to be involved in competing intra-chain interactions that lead to β-sheet-rich fibril formation *in vitro* (36). It is possible that SAF-93 is able to inhibit the fibril-promoting interactions between residues 104–122 and 129–141 that such studies with isolated peptides have indicated.

Very recently, Proske *et al.* (58) have isolated an aptamer to a peptide spanning residues 90–129 of PrP, which has the ability to reduce the level of PrP^{Sc} accumulation in persistently prion-infected neuroblastoma cells. It is intriguing that there is a potential overlap between the binding site of our SAF-93 and their aptamer DP7 (58). It should be noted, however, that region 90–129 includes part of the N-terminal, conformationally non-selective nucleic acid binding region of PrP (this study) and that these aptamers do not share any similarity in either the primary or the secondary structures. It remains to be determined whether DP7 aptamer exhibits any differential affinity between α-helix rich and β-oligomer PrP, as it was selected using a short peptide of undefined structure, rather than infectious material, as employed here. Furthermore, aptamer DP7 comprises pyryimidine 2′-amino, 2′-deoxyribonucleotides, rather than the 2′-F modifications employed in this work. It is known that different substitutions at the 2′-position result in changes in binding activity, probably by influencing the functional folding of RNA (29). It is significant that both aptamers were able to interfere with the conversion of PrP^{C} into PrP^{Sc}. Any comparison between the potency of the two aptamers in this regard must be made with caution, as the *in vitro* conversion assays were fundamentally different. Nevertheless, there is reason to believe that aptamer SAF-93, described here, may be the more potent inhibitor as it produced ~2-fold inhibition of conversion at 40 nM, compared with 700 nM, for comparable effects with DP7 (58).

Our data strengthen the existing literature about the intrinsic property of the α-helical form of PrP to interact with nucleic acids in general and RNA in particular, and extend the high affinity of the prion protein for RNA to the β-form disease-related PrP. These properties should be investigated further in order to gain more insight into the putative physiological role of PrP in RNA metabolism (25, 26, 28) and should provide ways to trap PrP in a disease-inactive conformation that might cleanse physiological fluids.

REFERENCES

1. Riek, R., Hornemann, S., Wider, G., Billeter, M., Glockshuber, R., and Wuthrich, K. (1996) *Nature* **382,** 180–182
2. Riek, R., Hornemann, S., Wider, G., Glockshuber, R., and Wuthrich, K. (1997) *FEBS Lett.* **413,** 282–288
3. Billeter, M., Riek, R., Wider, G., Hornemann, S., Glockshuber, R., and Wuthrich, K. (1997) *Proc. Natl. Acad. Sci. U. S. A.* **94,** 7281–7285
4. Riek, R., Wider, G., Billeter, M., Hornemann, S., Glockshuber, R., and Wuthrich, K. (1998) *Proc. Natl. Acad. Sci. U. S. A.* **95,** 11667–11672
5. Donne, D. G., Viles, J. H., Groth, D., Mehlhorn, I., James, T. L., Cohen, F. E., Prusiner, S. B., Wright, P. E., and Dyson, H. J. (1997) *Proc. Natl. Acad. Sci. U. S. A.* **94,** 13452–13457
6. James, T. L., Liu, H., Ulyanov, N. B., Farr-Jones, S., Zhang, H., Donne, D. G., Kaneko, K., Groth, D., Mehlhorn, I., Prusiner, S. B., and Cohen, F. E. (1997)

Proc. Natl. Acad. Sci. U. S. A. **94,** 10086–10091
7. Liu, H., Farr-Jones, S., Ulyanov, N. B., Llinas, M., Marqusee, S., Groth, D., Cohen, F. E., Prusiner, S. B., and James, T. L. (1999) *Biochemistry* **38,** 5362–5377
8. Lopez Garcia, F., Zahn, R., Riek, R., and Wuthrich, K. (2000) *Proc. Natl. Acad. Sci. U. S. A.* **97,** 8334–8339
9. Knaus, K. J., Morillas, M., Swietnicki, W., Malone, M., Surewicz, W. K., and Yee, V. C. (2001) *Nat Struct Biol.* **8,** 770–774
10. Zahn, R., Liu, A., Luhrs, T., Riek, R., von Schroetter, C., Lopez Garcia, F., Billeter, M., Calzolai, L., Wider, G., and Wuthrich, K. (2000) *Proc. Natl. Acad. Sci. U. S. A.* **97,** 145–150
11. Telling, G. C., Scott, M., Mastrianni, J., Gabizon, R., Torchia, M., Cohen, F. E., DeArmond, S. J., and Prusiner, S. B. (1995) *Cell* **83,** 79–90
12. Kaneko, K., Zulianello, L., Scott, M., Cooper, C. M., Wallace, A. C., James, T. L., Cohen, F. E., and Prusiner, S. B. (1997) *Proc. Natl. Acad. Sci. U. S. A.* **94,** 10069–10074
13. Hornshaw, M. P., McDermott, J. R., and Candy, J. M. (1995) *Biochem. Biophys. Res. Commun.* **207,** 621–629
14. Jobling, M. F., Huang, X., Stewart, L. R., Barnham, K. J., Curtain, C., Volitakis, I., Perugini, M., White, A. R., Cherny, R. A., Masters, C. L., Barrow, C. J., Collins, S. J., Bush, A. I., and Cappai, R. (2001) *Biochemistry* **40,** 8073–8084
15. Miura, T., Hori-i, A., Mototani, H., and Takeuchi, H. (1999) *Biochemistry* **38,** 11560–11569
16. Stockel, J., Safar, J., Wallace, A. C., Cohen, F. E., and Prusiner, S. B. (1998) *Biochemistry* **37,** 7185–7193
17. Brown, D. R., Hafiz, F., Glasssmith, L. L., Wong, B. S., Jones, I. M., Clive, C., and Haswell, S. J. (2000) *EMBO J.* **19,** 1180–1186
18. Caughey, B., Brown, K., Raymond, G. J., Katzenstein, G. E., and Thresher, W. (1994) *J. Virol.* **68,** 2135–2141
19. Warner, R. G., Hundt, C., Weiss, S., and Turnbull, J. E. (2002) *J. Biol. Chem.* **277,** 18421–18430
20. Brimacombe, D. B., Bennett, A. D., Wusteman, F. S., Gill, A. C., Dann, J. C., and Bostock, C. J. (1999) *Biochem. J.* ***342 Pt*** **3,** 605–613
21. Sklaviadis, T., Akowitz, A., Manuelidis, E. E., and Manuelidis, L. (1993) *Proc. Natl. Acad. Sci. U. S. A.* **90,** 5713–5717
22. Akowitz, A., Sklaviadis, T., and Manuelidis, L. (1994) *Nucleic Acids Res.* **22,** 1101–1107
23. Nandi, P. K. (1998) *Arch Virol.* **143,** 1251–1263
24. Cordeiro, Y., Machado, F., Juliano, L., Juliano, M. A., Brentani, R. R., Foguel, D., and Silva, J. L. (2001) *J. Biol. Chem.* **276,** 49400–49409
25. Gabus, C., Auxilien, S., Pechoux, C., Dormont, D., Swietnicki, W., Morillas, M., Surewicz, W., Nandi, P., and Darlix, J. L. (2001) *J. Mol. Biol.* **307,** 1011–1021
26. Gabus, C., Derrington, E., Leblanc, P., Chnaiderman, J., Dormont, D., Swietnicki, W., Morillas, M., Surewicz, W. K., Marc, D., Nandi, P., and Darlix, J. L. (2001) *J. Biol. Chem.* **276,** 19301–19309
27. Weiss, S., Proske, D., Neumann, M., Groschup, M. H., Kretzschmar, H. A., Famulok, M., and Winnacker, E. L. (1997) *J. Virol.* **71,** 8790–8797
28. Moscardini, M., Pistello, M., Bendinelli, M., Ficheux, D., Miller, J. T., Gabus, C., Le Grice, S. F., Surewicz, W. K., and Darlix, J. L. (2002) *J. Mol. Biol.* **318,** 149–159
29. Tahiri-Alaoui, A., Frigotto, L., Manville, N., Ibrahim, J., Romby, P., and James, W. (2002) *Nucleic Acids Res.* **30,** e45
30. Heidenreich, O., Kang, S. H., Brown, D. A., Xu, X., Swiderski, P., Rossi, J. J., Eckstein, F., and Nerenberg, M. (1995) *Nucleic Acids Res.* **23,** 2223–2228
31. Kimberlin, R. H., and Walker, C. A. (1978) *J. Gen. Virol.* **39,** 487–496
32. Hope, J., Morton, L. J., Farquhar, C. F., Multhaup, G., Beyreuther, K., and Kimberlin, R. H. (1986) *EMBO J.* **5,** 2591–2597
33. Jackson, G. S., Hill, A. F., Joseph, C., Hosszu, L., Power, A., Waltho, J. P., Clarke, A. R., and Collinge, J. (1999) *Biochim. Biophys. Acta.* **1431,** 1–13
34. Adams, T. E., MacIntosh, B., Brandon, M. R., Wordsworth, P., and Puri, N. K. (1992) *Gene* (*Amst.*) **122,** 371–375
35. Baskakov, I. V., Legname, G., Baldwin, M. A., Prusiner, S. B., and Cohen, F. E. (2002) *J. Biol. Chem.* **277,** 21140–21148
36. Tahiri-Alaoui, A., Bouchard, M., Zurdo, J., and James, W. (2003) *Protein Sci.* **12,** 600–608
37. Laemmli, U. K. (1970) *Nature* **227,** 680–685
38. Towbin, H., Staehelin, T., and Gordon, J. (1979) *Proc. Natl. Acad. Sci. U. S. A.* **76,** 4350–4354
39. Kirby, L., Birkett, C. R., Rudyk, H., Gilbert, I. H., and Hope, J. (2003) *J. Gen. Virol.* **84,** 1013–1020
40. Horiuchi, M., and Caughey, B. (1999) *Struct. Fold Des.* **7,** R231–240
41. Tuerk, C. (1997) *Methods Mol. Biol.* **67,** 219–230
42. Baskakov, I. V., Legname, G., Prusiner, S. B., and Cohen, F. E. (2001) *J. Biol. Chem.* **276,** 19687–19690
43. Hornemann, S., Korth, C., Oesch, B., Riek, R., Wider, G., Wuthrich, K., and Glockshuber, R. (1997) *FEBS Lett.* **413,** 277–281
44. Supattapone, S., Bosque, P., Muramoto, T., Wille, H., Aagaard, C., Peretz, D., Nguyen, H. O., Heinrich, C., Torchia, M., Safar, J., Cohen, F. E., DeArmond, S. J., Prusiner, S. B., and Scott, M. (1999) *Cell* **96,** 869–878
45. Peretz, D., Williamson, R. A., Matsunaga, Y., Serban, H., Pinilla, C., Bastidas, R. B., Rozenshteyn, R., James, T. L., Houghten, R. A., Cohen, F. E., Prusiner, S. B., and Burton, D. R. (1997) *J. Mol. Biol.* **273,** 614–622
46. Brown, D. R. (2000) *Biochem. J.* ***346,*** 785–791
47. Gu, Y., Fujioka, H., Mishra, R. S., Li, R., and Singh, N. (2002) *J. Biol. Chem.* **277,** 2275–2286
48. Ettaiche, M., Pichot, R., Vincent, J. P., and Chabry, J. (2000) *J. Biol. Chem.* **275,** 36487–36490
49. Rymer, D. L., and Good, T. A. (2000) *J Neurochem.* **75,** 2536–2545
50. Singh, N., Gu, Y., Bose, S., Kalepu, S., Mishra, R. S., and Verghese, S. (2002) *Front. Biosci.* **7,** a60–71
51. Turk, E., Teplow, D. B., Hood, L. E., and Prusiner, S. B. (1988) *Eur. J. Biochem.* **176,** 21–30
52. Wille, H., Michelitsch, M. D., Guenebaut, V., Supattapone, S., Serban, A., Cohen, F. E., Agard, D. A., and Prusiner, S. B. (2002) *Proc. Natl. Acad. Sci. U. S. A.* **99,** 3563–3568
53. Steitz, T. A. (1999) in *The RNA World* (Gesteland, R. F., Cech, T, R, and Atkins, J. F., eds) 2nd Ed., pp. 427–450, Cold Spring Harbor Laboratory, New York
54. Horiuchi, M., Priola, S. A., Chabry, J., and Caughey, B. (2000) *Proc. Natl. Acad. Sci. U. S. A.* **97,** 5836–5841
55. Caughey, B. W., Dong, A., Bhat, K. S., Ernst, D., Hayes, S. F., and Caughey, W. S. (1991) *Biochemistry* **30,** 7672–7680
56. Pan, K. M., Baldwin, M., Nguyen, J., Gasset, M., Serban, A., Groth, D., Mehlhorn, I., Huang, Z., Fletterick, R. J., Cohen, F. E., and Prusiner, S. B. (1993) *Proc. Natl. Acad. Sci. U. S. A.* **90,** 10962–10966
57. Kocisko, D. A., Lansbury, P. T., Jr., and Caughey, B. (1996) *Biochemistry* **35,** 13434–13442
58. Proske, D., Gilch, S., Wopfner, F., Schatzl, H. M., Winnacker, E. L., and Famulok, M. (2002) *Chembiochem.* **3,** 717–725